Radioiodinated *N*-(2-Diethylaminoethyl)benzamide Derivatives with High Melanoma Uptake: Structure−Affinity Relationships, Metabolic Fate, and Intracellular Localization

Michael Eisenhut,* William E. Hull,† Ashour Mohammed, Walter Mier, Dorothee Lay,‡ Wilhelm Just,‡ Karin Gorgas,# Wolf D. Lehmann,† and Uwe Haberkorn

Department of Nuclear Medicine, Center of Biochemistry, and Institute for Anatomy and Cell Biology, University of Heidelberg, D-69120 Heidelberg, Germany, and Central Spectroscopy Department, German Cancer Research Center (DKFZ), Heidelberg, Germany

Received May 11, 1999

Several radioiodinated *N*-(dialkylaminoalkyl)benzamides have been used for planar scintigraphy and single-photon emission computed tomography (SPECT) of melanoma metastases. In a quest for improved melanoma uptake and tissue selectivity, structure−activity studies for *N*-(2-diethylaminoethyl)benzamides with variation of phenyl substituents were performed using C57Bl/6 mice bearing B16 melanoma. Compounds **2** (4-amino-5-bromo-*N*-(2-diethylaminoethyl)-3-[^{131}I]iodo-2-methoxybenzamide) and **6** (4-acetamido-*N*-(2-diethylaminoethyl)-5-[^{131}I]iodo-2-methoxybenzamide) showed at 6 h post iv injection, for example, melanoma uptake of 16.6 and 23.2% ID/g, respectively (mean values, $n = 3$). Uptake was 3−5 times higher ($P < 0.01$) than observed with benzamides known from the literature and was probably facilitated by the relatively slow urinary excretion of **2** or **6**. In contrast, analogues lacking either the MeO, Ac, AcNH, or Br substituents exhibited reduced tumor uptake and high urinary excretion of radioactivity in various benzamide metabolites. Uptake of radioiodinated benzamides in B16 melanoma is not mediated by a specific mechanism such as σ-receptor binding. **2** and **6** exhibited similar melanoma uptake values but quite different σ_1-receptor affinities of $K_i = 0.278 \pm 0.018$ and 5.19 ± 0.40 μM, respectively. Uptake studies with IMBA (*N*-(2-diethylaminoethyl)-3-[^{131}I]-iodo-4-methoxybenzamide) or BZA (*N*-(2-diethylaminoethyl)-4-[^{131}I]iodobenzamide) showed that with increasing dose of unlabeled compound the measured uptake of label was unchanged (IMBA) or even enhanced (BZA) while receptor binding of label decreased. Differential and equilibrium density-gradient centrifugation revealed that most of the radioactivity from labeled IMBA was associated with fractions containing melanin granules. Thus, structure−activity studies indicate that blood clearance rates and metabolic stability are the main determinants for benzamide uptake in melanoma. The high uptake and slow clearance of **6** offer considerable potential for melanoma imaging in patients, and this compound may also prove to be useful for radionuclide therapy.

Introduction

The ability of melanoma metastases to disseminate rapidly means that early detection is an important diagnostic goal for the successful treatment and followup of patients. Therefore, the development of an effective radiopharmaceutical with melanoma affinity has been pursued for some time. The discovery of radioiodinated benzamides which exhibit affinity to melanocytes led to the development of several *N*-(2-dialkylaminoalkyl)-4-iodobenzamide derivatives. Their remarkable affinity was accidentally observed as uveal uptake in pigmented experimental animals.[1] The evaluation of structural variations in benzamide derivatives in terms of their biological behavior in melanoma-bearing mice focused primarily on amide substituents and the position of radioiodine in the phenyl ring.[2−4] Introduction of a polar phenyl substituent such as 4-MeO in IMBA (*N*-(2-diethylaminoethyl)-3-[^{123}I]iodo-4-methoxybenzamide) resulted in faster clearance from nontarget tissue than obtained with BZA (*N*-(2-diethylaminoethyl)-4-[^{123}I]iodobenzamide) and improved contrast in scintigraphic images of melanoma patients.[5] A subsequent systematic investigation of the influence of the phenyl substituents HO, MeO, and H_2N on melanoma uptake and pharmakokinetics in mice led to several derivatives with characteristics similar to but not better than those of IMBA.[6]

In our continuing efforts to improve scintigraphic tumor contrast by modifying the benzamide structures, we synthesized a series of compounds which may enhance our understanding of the influence of phenyl substituents on melanoma uptake. Some of the new benzamide derivatives exhibited much higher affinity for melanoma tissue than observed with the benzamides known from the literature and our own previous work. This paper reports the synthesis, characterization, and biological evaluation of these new compounds with emphasis on structure−activity relationships (SAR),

* To whom correspondence should be addressed. Tel: ++49-6221-567720. Fax: ++49-6221-565473. E-mail: michael_eisenhut@med.uni-heidelberg.de.
† German Cancer Research Center.
‡ Center of Biochemistry.
§ Institute for Anatomy and Cell Biology.

10.1021/jm991079p CCC: $19.00
Published on Web 09/26/2000

Scheme 1[a]

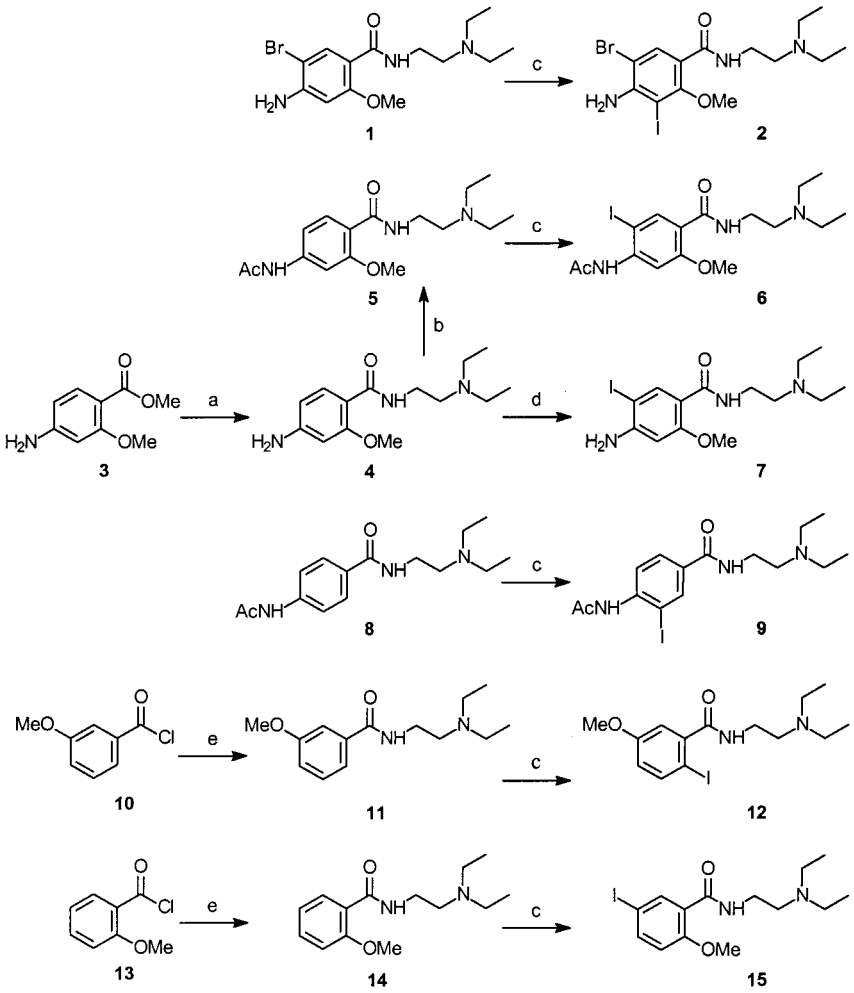

[a] Reaction conditions: (a) 2-diethylaminoethylamine, 90 °C/12 h; (b) AcCl, 25 °C/1 h; (c) $Tl(TFA)_3$/TFA, 25 °C/30 min, and I^-, 25 °C/5 h or $^{131}I^-$, 25 °C/5 min; (d) KIO_3/I^-, 25 °C/30 min or $KIO_3/^{131}I^-$, 25 °C/10 min; (e) 2-diethylaminoethylamine, 25 °C/2 h.

where activity refers to melanoma affinity in our context. In addition, the biological mechanisms which may influence scintigraphic contrast in clinical studies were investigated by tracing the metabolic fate of [^{123}I]-IMBA[5] and [^{123}I]BZA.[7] Finally, to learn more about the binding and cellular localization of the benzamides, e.g., the importance of σ_1-receptors versus melanin, we performed in vitro receptor binding studies and in vivo saturation studies and investigated the intracellular distribution of the benzamides in melanoma cells by density-gradient centrifugation measurements.

Results

Chemistry. The syntheses of the benzamides **2**, **6**, **7**, **9**, **12**, and **15** and their radioiodinated analogues were accomplished by the routes outlined in Scheme 1. For **2** the commercially available bromopride **1** was regioselectively iodinated by replacing a bis(trifluoroacetyl)-thallium group generated in situ at the benzamide C3 position with iodine.[5,6] Thallation, without separation of products, and iodination were performed at ambient temperature. The synthesis of **6** was started with the aminolysis of methyl 4-amino-2-methoxybenzoate (**3**) using excess 2-diethylaminoethylamine. Subsequent reaction of compound **4** with acetyl chloride afforded precursor **5** which was thallated and iodinated as described above. **7** was obtained by adding an aqueous iodide solution to an equimolar mixture of precursor **4** and KIO_3 in HCl. *N*-Acetylprocainamide **8** was iodinated with $Tl(TFA)_3/I^-$ as described above to give **9**. **12** was synthesized by the reaction of 3-methoxybenzoyl chloride (**10**) with 2-diethylaminoethylamine to give benzamide **11**. The corresponding 2-iodo-5-methoxy derivative **12** was obtained by iodination with $Tl(TFA)_3/I^-$ as described above. **15** was synthesized in a similar manner; the corresponding acid chloride **13** was reacted with excess 2-diethylaminoethylamine to give the amide **14** which was iodinated with $Tl(TFA)_3/I^-$. Purification was performed by recrystallization until HPLC indicated >95% purity. The complete and unambiguous structural identification of the various benzamides was only possible through the use of both ^{1}H and ^{13}C NMR (Tables 5 and 6). Although many of the signal assignments (numbering given in Chart 1) for the one-dimensional spectra could be tentatively made using chemical shift predictions, a definitive determination of the phenyl ring substitution pattern required the a priori positional assignments for all carbons via long-range couplings to protons. Therefore, for several compounds the fully ^{1}H-coupled ^{13}C NMR spectrum was acquired and, where necessary, ^{13}C NMR spectra with selective ^{1}H decou-

Chart 1. Numbering for the Signal Assignments in ^{1}H and ^{13}C NMR Spectra of **2**, **6**−**9**, **12**, and **15** (Tables 5 and 6)

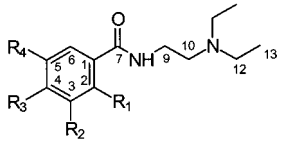

pling and ^{1}H−^{1}H nuclear Overhauser effects (NOE) were examined.

For the analogous radioiodination reactions the molar amounts of the precursors were reduced so that the complete reaction mixture could be separated on an analytical RP-18 column. Excellent radiochemical yields were obtained with the Tl(TFA)$_3$/^{131}I$^-$ and KIO$_3$/^{131}I$^-$ methods (70−90%). Specific activities of the radioiodinated benzamides **2**−**15** were in the range 65−90 Gbq/μmol.

Biodistribution Studies. To judge their potential as tumor markers, the ^{131}I-labeled benzamides **2**, **6**, **7**, **9**, **12**, and **15** were injected intravenously into C57Bl/6 mice bearing subcutaneously transplanted B16 melanoma. Time points of 1 and 6 h after injection were chosen for determining the distribution of each compound in various organs and tissues. For those benzamides with high melanoma uptake, a 24-h time point was included to judge long-term retention. The biodistribution data are summarized in Table 1.

The benzamides **2** and **6** exhibited the highest melanoma uptake and excellent retention. At 1 h the uptake was 17 and 22% ID/g, respectively, with average melanoma/nontarget tissue ratios (M/NTT, selectivity parameter) of 9 and 10. At 6 h tumor content was essentially unchanged, and M/NTT increased to 25 and 30, respectively. After 24 h the radioactivity in tumor decreased to ca. 8 and 16% ID/g while clearance from other tissues (except liver) was high, yielding M/NTT values of 132 (**2**) and 251 (**6**).

The influence of the phenyl ring substituents on tissue uptake is reflected by the results for **2** and **6** in comparison with the other benzamide derivatives in Table 1. The following structural changes led to a significant ($P < 0.001$) absolute decline in melanoma uptake: (1) 5-Br → 5-I and 3-I → 3-H (**2** → **7**); (2) 4-AcNH → 4-NH$_2$ (**6** → **7**); (3) 2-OMe → 2-H (**6** → **9**); (4) 4-AcNH → 4-H (**6** → **15**). Additionally, the M/NTT ratios (selectivity) also decreased for the changes listed above, except for **6** → **15**.

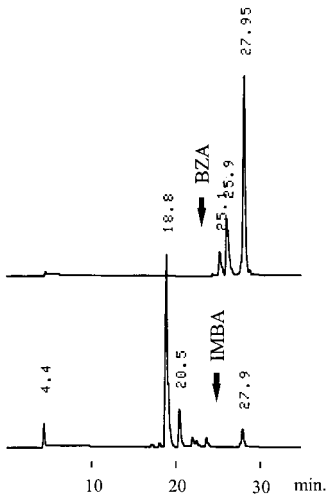

Figure 1. γ-HPLC of urine collected for 4 h after injecting [^{131}I]IMBA (lower panel) or [^{131}I]BZA (upper panel) into C57Bl/6 mice. Arrows indicate the retention times of the original compounds.

The benzamides **12**−**15** were also compared with IMBA[5] to learn whether the positions of radioiodine and the methoxy group can be optimized. For example, for the rearrangement 3-I → 2-I and 4-OMe → 5-OMe (IMBA → **12**), melanoma uptake increased slightly at 1 h but decreased slightly at 6 h (one-sided $P = 0.08$ in both cases) while selectivity decreased, especially at 6 h. For the rearrangement to 2-OMe, 5-I (**15**) there was little improvement in absolute uptake at 1 h (one-sided $P = 0.1$) and a small improvement at 6 h (one-sided $P = 0.06$) compared to IMBA, but selectivity was poorer.

Urinary Metabolites of Benzamides. In view of the significant differences in the biodistribution of the benzamides, we investigated the metabolic fate of some of these compounds (IMBA, BZA, **2**, **6**, and **15**). After iv injection of a given ^{131}I-labeled benzamide into C57Bl/6 mice, urine was collected for 4 h and analyzed by RP-HPLC. The elution profiles for ^{131}I-labeled IMBA and BZA are shown in Figure 1, and the differences observed indicate that these two compounds follow different metabolic routes. While IMBA was mainly transformed

Table 1. Biodistribution of Radioiodinated *N*-(2-Diethylamino)benzamides **2**−**15** in C57Bl/6 Mice with B16 Melanoma

	phenyl substituent position				time (h,		mean tissue concentrations (% ID/g, $n = 3$)[a]								
compd	2	3	4	5	postinject)	M/NTT[b]	melanoma	blood	heart	lung	spleen	liver	kidney	muscle	brain
2	MeO	I	NH$_2$	Br	1	9	16.61 ± 1.44	2.32 ± 0.06	1.91	3.16	5.06	11.32	4.53	0.94	0.64
					6	25	16.48 ± 0.46	1.86 ± 0.61	0.94	2.07	1.84	9.61	2.08	0.43	0.15
					24	132	8.02 ± 0.69	0.19 ± 0.05	0.13	0.26	0.38	4.54	0.46	0.01	0.02
6	MeO	H	AcNH	I	1	10	21.87 ± 0.43	3.30 ± 0.56	2.10	5.53	6.55	8.03	5.09	1.37	0.62
					6	30	23.32 ± 0.36	2.56 ± 1.23	1.05	3.02	2.09	9.86	1.97	0.44	0.19
					24	251	16.06 ± 1.25	0.21 ± 0.00	0.09	0.25	0.17	3.72	0.40	0.03	0.02
7	MeO	H	NH$_2$	I	1	6	4.66 ± 0.29	1.93 ± 0.08	1.17	3.12	2.00	4.92	6.89	0.61	0.18
					6	19	6.92 ± 0.85	0.85 ± 0.59	0.45	1.06	1.57	3.43	3.95	0.28	0.08
9	H	I	AcNH	H	1	3	6.21 ± 1.29	6.50 ± 0.73	3.19	7.98	5.62	4.05	6.46	1.81	0.48
					6	3	1.20 ± 0.12	1.51 ± 0.38	0.58	1.82	1.39	0.77	1.22	0.44	0.09
12	I	H	H	MeO	1	15	8.06 ± 1.22	0.90 ± 0.16	0.63	1.41	1.26	1.23	1.81	0.38	0.15
					6	24	2.32 ± 0.87	0.33 ± 0.23	0.13	0.41	0.31	0.23	0.17	0.08	0.02
15	MeO	H	H	I	1	14	7.73 ± 1.08	0.46 ± 0.06	0.46	1.15	2.50	0.88	1.71	0.19	0.50
					6	73	6.80 ± 1.53	0.14 ± 0.06	0.09	0.19	0.15	0.26	0.41	0.04	0.04
IMBA[c]	H	I	MeO	H	1	24	6.50 ± 0.44	0.20 ± 0.10	0.25	0.69	0.39	2.62	0.93	0.19	0.10
					6	129	4.14 ± 1.20	0.04 ± 0.00	0.05	0.09	0.05	0.29	0.17	0.03	0.01

[a] To simplify the table, standard deviations are shown only for melanoma and blood data. [b] Selectivity parameter calculated as the mean of 8 melanoma/nontarget tissue ratios. [c] From ref 5.

Table 2. Excretion of Radioactivity into Urine[a]

compd	4-h urine[b]	comparison (*P* value)[c]
2	34 ± 6	**6** (0.01)
6	16 ± 3	
15	71 ± 5	**2** (0.001)
BZA	66 ± 5	**2** (0.005)
IMBA	82 ± 8	**2** (<0.001)
		15 (0.05)

[a] NMRI mice. [b] % ID, mean ± SD (3 animals). [c] *P* value for comparison of means (one-sided *t*-test with equal variance).

Table 3. Receptor Binding Data and Partition Coefficients for Benzamides **2**−**15**[a]

	K_i (nM)		
compd	σ_1-receptor[b]	σ_2-receptor[c]	log *P*,[d] pH 7.4
2	278 ± 18	2350 ± 65	1.81 ± 0.11
6	5190 ± 397	115000 ± 18200	1.78 ± 0.01
7	484 ± 27	21400 ± 17800	1.62 ± 0.02
9	4645 ± 508	148000 ± 30800	1.34 ± 0.09
12	455 ± 35	347 ± 23	1.16 ± 0.02
15	92 ± 8	1020 ± 91	1.26 ± 0.02
IMBA	249 ± 17	6520 ± 360	1.13 ± 0.01
haloperidol	2.95 ± 0.58	46.5 ± 2.1	

[a] Results represent mean ± SD for 2−4 measurements. [b] Competition assay with guinea pig brain membranes and [^{3}H]-(+)-pentazocine as ligand. [c] Rat liver membranes with [^{3}H]DTG as ligand. [d] Octanol/water partition coefficient.

to a more polar metabolite, BZA was converted to a more lipophilic compound. The urinary metabolite pattern for **15** was nearly identical to that for IMBA. In contrast, the highly accumulating benzamides **2** and **6** were excreted to a lesser extent. As summarized in Table 2, the amount of urinary radioactivity collected within 4 h after injection was lowest with **6** and **2**: i.e., only about one-fourth or one-half, respectively, of the excretion observed with benzamide **15**, BZA, or IMBA. For **2** and **6** HPLC analysis of the urine samples revealed that the radioactivity was almost exclusively in the form of [^{131}I]-iodide.

The main metabolites of BZA and IMBA were identified by injecting 1 mg of the unlabeled benzamide into C57Bl/6 mice. Urine was collected for 4 h postinjection, and desalted samples were analyzed by negative-ion ESI-MS/MS. The $[I]^-$ fragment at *m*/*z* 126.9 was used for a parent-ion scan to detect only iodinated species. The main metabolites of IMBA were identified as the sulfate (*m*/*z* 441) and glucuronate (*m*/*z* 537) of *N*-(2-diethylaminoethyl)-4-hydroxy-3-iodobenzamide. 4-Iodohippuric acid (*m*/*z* 304) and an unknown metabolite (*m*/*z* 483) were detected using BZA.

Partition Coefficients. The lipophilicities were measured by partitioning no-carrier-added radioiodinated benzamides **2**, **6**, **7**, **9**, **12**, and **15** and IMBA in an 1-octanol/buffer system at pH 7.4. The results are summarized in Table 3. The log *P* values fall into two groups with ranges of 1.6−1.9 (**2**, **6**, and **7**) and 1.1−1.3 (**9**, **12**, **15**, and IMBA).

Receptor Binding Studies. The IC_{50} values for the binding of unlabeled benzamides **2**−**15** to σ-receptors were determined by means of competitive binding assays, using guinea pig brain membranes (σ_1-receptors) with the ligand [^{3}H]-(+)-pentazocine[8] and rat liver membranes (σ_2-receptors) with [^{3}H]DTG.[9] The apparent K_d values for the radioligands were 6.44 ± 0.53 nM (σ_1) and 23.7 ± 2.0 nM (σ_2), respectively. K_i values for the benzamides were calculated using the Cheng−Prusoff equation,[10] and the results are summarized in Table 3. The inhibition potency of the benzamides varied considerably. Moderate affinities for σ_1-receptors were obtained with **2**, **7**, **12**, **15**, and IMBA. Their K_i values ranged from 92 nM (**15**) to 484 nM (**7**), while **6** and **9** exhibited K_i values of about 5 μM. In general, the benzamides proved to be relatively poor ligands for σ_2-receptors (K_i > 1 μM), with the exception of **12** (K_i = 347 nM).

The expression of σ-receptors in B16 melanoma cells was investigated by saturating tumor cell membranes with [^{3}H]-(+)-pentazocine and [^{3}H]DTG. The cell membranes (P2 pellet) were obtained from C57Bl/6 mice with subcutanously transplanted B16 melanoma. To avoid complications with necrotic tissue, cells were harvested from small tumors weighing 0.1−0.25 g. Tissue affinity for ^{131}I-labeled benzamides was tested with [^{131}I]**2** and found to be consistent with the uptake data listed in Table 1: i.e., 14.2% ID/g at 1 h after injection. The K_d values of [^{3}H]-(+)-pentazocine (σ_1) and [^{3}H]DTG/dextrallorphan (σ_2) obtained with B16 melanoma membranes were 109 ± 33 nM (B_{max} = 23200 ± 4200 fmol/mg) and 101 ± 25 nM (B_{max} = 18700 ± 2670 fmol/mg), respectively.

In Vivo Saturation Experiments. Additional information about the binding of radioiodinated benzamides in B16 cells as a function of specific activity was obtained by injecting C57Bl/6 mice with a constant amount of radioiodinated IMBA or BZA together with increasing amounts of the unlabeled compound. The biodistribution data for melanoma and blood are summarized in Table 4. The melanoma content of labeled IMBA showed little change with decreasing specific activity, while the uptake of labeled BZA actually increased with the addition of unlabeled compound and with time (6 h vs 1 h). Increasing amounts of unlabeled IMBA and BZA injected into the animals altered the M/NTT ratios (specificity) differently. The ratios increased using BZA and were reduced with IMBA. The reduction of IMBA specificity passed, however, not below the ratios obtained with no-carrier-added [^{131}I]-BZA.

Intracellular Distribution of [^{131}I]IMBA in B16 Melanoma. After exposure to [^{131}I]IMBA excised tumor tissue was homogenized, and the homogenate was fractionated by differential centrifugation (Figure 2A). A sample of the unfractionated homogenate as well as pellets 2 and 3 obtained by differential centrifugation and sedimentation at 3500*g* and 14000*g*, respectively, were further analyzed by equilibrium density-gradient centrifugation (Figure 2B). The measured distribution of radioactivity revealed that the majority of [^{131}I]IMBA (more than 60% in fractions 1−4) sedimented to a high equilibrium density (1.26 g/mL), beyond that of peroxisomes which usually are recovered at densities of 1.22−1.23 g/mL. This result indicates that [^{131}I]IMBA cosediments with melanin granules which are known to exhibit buoyant densities of about 1.26 g/mL in a sucrose gradient.[11] Finally, the organelles were recovered from the peak fractions with the highest content of [^{131}I]-IMBA, and ultrastructural analysis was performed. Figure 2C shows the subcellular composition of fraction 2, demonstrating that the majority of structures present were melanin granules.

Table 4. Influence of Carrier Addition on Melanoma Uptake and Blood Values of Labeled Benzamide[a]

compd	total BA injected (μmol/mouse)	melanoma (% ID/g)		blood (% ID/g)		M/NTT[b]	
		1 h	6 h	1 h	6 h	1 h	6 h
IMBA	1.8×10^{-6}	6.50 ± 0.44	4.14 ± 1.20	0.20 ± 0.10	0.04 ± 0.00	24	129
	1.5×10^{-3}	4.86 ± 0.56	5.27 ± 0.49	1.03 ± 0.04	0.24 ± 0.08	10	88
	1.5	5.41 ± 0.43	3.72 ± 0.54	0.78 ± 0.26	0.29 ± 0.11	10	48
BZA	3.9×10^{-7}	5.67 ± 0.45	9.32 ± 0.21	0.65 ± 0.04	0.17 ± 0.03	3	27
	2.0×10^{-3}	10.02 ± 0.48[c]	15.47 ± 0.73[c]	1.06 ± 0.36	0.15 ± 0.03	4	50
	1.7	11.60 ± 0.60[d]	14.58 ± 1.47[d]	1.04 ± 0.19	0.10 ± 0.04	5	45

[a] Mean ($n = 3$). [b] Selectivity parameter calculated as the mean of 8 melanoma/nontarget tissue ratios. [c] $P < 0.01$. [d] $P < 0.05$ (in comparison with no-carrier-added injection).

Discussion

For the radioiodinated *N*-(2-diethylaminoethyl)benzamide derivatives discussed up to now in the literature, diverse values of melanoma uptake have been observed. In our current study of B16 melanoma in the C57Bl/6 mouse (Table 1), benzamides **2** and **6** exhibited the highest uptake at 1 and 6 h postinjection with a 3−5-fold increase compared to radioiodinated IMBA, a recently developed benzamide with improved scintigraphic contrast.[5] **2** and **6** also have the advantage of slow clearance from melanoma, with tumor levels decreasing from 6 to 24 h postinjection by only about 50% or 30%, respectively. Thus, tumor selectivity, expressed as the mean of the eight measured melanoma/nontarget tissue ratios (M/NTT), increased with time, reaching values of about 130 or 250, respectively, 1 day after injection.

Although IMBA exhibits only moderate melanoma uptake, comparable to that observed for several other benzamides in this study, it has the advantage of much faster clearance from nontarget tissues, including the liver, so that M/NTT reaches about 130 after only 6 h. Thus, IMBA can provide the highest scintigraphic contrast for melanoma metastases[5] at early times postinjection, but **2** or **6** can provide a significant improvement in sensitivity while reaching similar contrast ratios ca. 24 h after injection. A possible disadvantage of **2** and **6** is their relatively high uptake in the liver and slow clearance from that organ (melanoma/liver ratios at 24 h are only 1.8 and 4.3, respectively).

Role of Metabolism and Renal Clearance. In the course of investigations aimed at improving the biological characteristics of IMBA, derivatives with the iodo and methoxy substituents at different positions in the phenyl ring have been prepared. Thus, 2-methoxy-5-iodophenyl substitution (**15**) led to a small increase in melanoma uptake (19% at 1 h and 64% at 6 h postinjection), but selectivity in terms of melanoma/nontarget tissue ratios decreased, except for liver and muscle. The opposite arrangement of phenyl substituents (2-iodo-5-methoxy in **12**) led to uptake and selectivity characteristics that were similar to those of IMBA at 1 h but significantly poorer at 6 h. On the other hand, when the phenyl substituents of **2** or **6** were altered or removed, absolute uptake into melanoma was reduced to levels similar to those observed for IMBA, and in some cases selectivity was also decreased. For example, loss of the acetyl group on the amine function at C4 (**7**) reduced uptake and to some extent selectivity. Loss of the methoxy group at C2 and the halogen at C5 (**9**) reduced uptake and increased clearance from tumor with a dramatic loss of selectivity at 6 h postinjection.

Thus, we find that the nature and position of phenyl substituents in the benzamide derivatives have a significant influence on their biodistribution and usefulness as melanoma markers. Possible mechanisms for these SAR effects could involve (1) efficiency of transport to the target tissue or binding site, (2) relative affinities at target and nontarget binding sites, or (3) rates of metabolism and renal clearance which influence intravasal bioavailability. On the basis of the large amount of data available from previous investigations,[5,6] it is likely that the third group of mechanisms is primarily responsible for the observed effects. From Tables 1 and 2 we see that **6**, which exhibits the highest uptake in tumor and several other tissues, also has the lowest clearance of radioactivity into the urine. For **2** melanoma uptake is somewhat lower while renal clearance is somewhat higher. In both of these cases urinary radioactivity was found to be primarily [^{131}I]iodide (I^-). These results are consistent with the hypothesis that in the absence of efficient metabolic pathways renal clearance is slow, resulting in high intravasal bioavailability, high uptake, and relatively slow clearance from all tissues but especially from melanoma. The relatively high partition coefficients (lipophilicity) observed for **2** and **6** (ca. 1.8, see Table 3) may also contribute to their favorable uptake.

In contrast, benzamide derivatives which can be efficiently metabolized may show more rapid clearance from tissues and higher radioactivity excretion rates. Metabolism has been proven for BZA (conversion to 4-iodohippuric acid by amide bond cleavage and formation of the glycine conjugate), IMBA (conversion to the 4-sulfate ester and 4-glucuronate), and **15** (metabolites not shown but similar to those of IMBA). Thus, metabolism is likely to be responsible for the relatively rapid nontarget tissue clearance observed for **15** and IMBA in Table 1 (especially from liver, spleen, and kidney) and the high renal clearance (Table 2) observed for all three compounds. Furthermore, blood levels at 1 or 6 h for the compounds listed in Table 2 were inversely correlated with the 4-h urinary excretion data. All of these results point to intravascular concentration as a major determinant of melanoma uptake. This conclusion is supported by the results of Figure 3, where melanoma tissue concentrations (radioactivity) at 1 h postinjection are plotted against blood concentrations for all compounds in Table 1. With the exception of compound **9**, the data show a modest linear correlation ($r = 0.85$), indicating that melanoma uptake is roughly proportional to the concentration of benzamide circulating in the blood. Thus, differences in the biodistribution data for the benzamide derivatives of Table 1 reflect differences in the routes of metabolic degradation and the

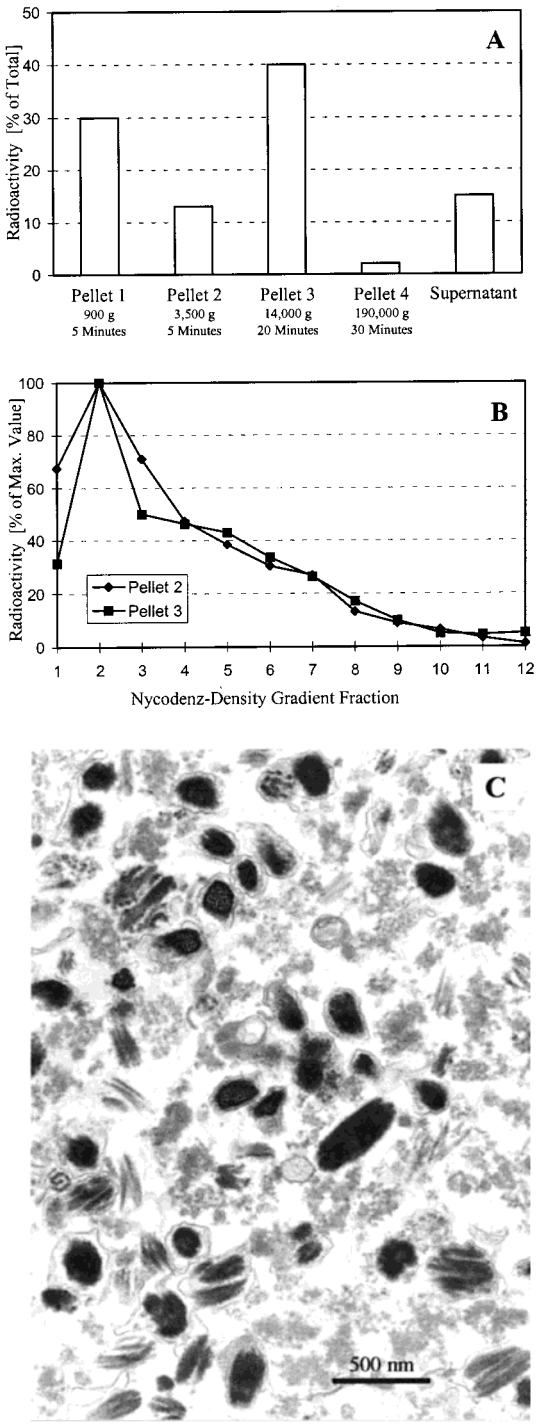

Figure 2. A: Distribution of radioactivity obtained by differential centrifugation of melanoma tissue homogenate. Pellets: (1) nuclei, debris; (2) peroxisomes, mitochondria, melanin granules; (3) lysosomes, melanin granules; (4) microsomes; (supernatant) soluble proteins, etc. B: Distribution of radioactivity in fractions obtained from density-gradient centrifugation (30−70% Nycodenz gradient) of pellets 2 and 3 obtained from differential centrifugation; melanosomes sediment in fractions 2−3. C: Subcellular composition of fraction 2 showing melanin granules.

rates of tissue and renal clearance of metabolites, which compete with melanoma uptake by reducing intravascular concentrations.

However, in Figure 3 we find that compound **9**, which lacks substituents at C2 and C5, represents a unique exception to the pattern of behavior exhibited by the

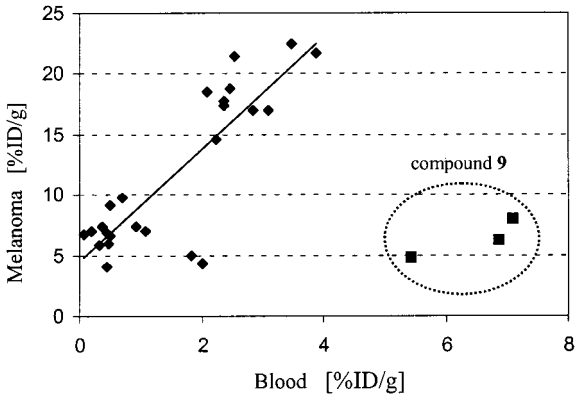

Figure 3. Correlation plot for benzamide uptake in melanoma tissue vs blood concentration at 1 h after injection of radioiodinated **2**, **6**, **7**, **9**, **12**, **15**, and IMBA. Each data point represents one animal and compound. The linear regression ($r = 0.85$) is for all data points except those for **9**.

other benzamides. Uptake at 1 h postinjection is similar for tumor, lung, spleen, liver, and kidney and about equal to the blood level; uptake is lower in heart, muscle, and expecially brain. At 6 h all tissue levels decrease in parallel with the blood level by about a factor of 4−5. Thus, **9** exhibits no selectivity for melanoma compared to several other important organs, and the data suggest that there is a rapid equilibrium between extravascular tissue and the intravascular volume.

Role of σ-Receptors. Radioiodinated *N*-(2-diethylaminoethyl)benzamide derivatives have been described to exhibit high affinity for the σ_1-receptor[2,12] expressed by several tumors.[13] As summarized in Table 3 the benzamides investigated here showed high to moderate σ_1-receptor affinities in vitro (K_i range: 92−5190 nM) which, however, do not correlate with the melanoma uptake values in Table 1 (range: 4.7−23.3% ID/g at 1 h postinjection). The *N*-acetylated derivative **6** exhibited the lowest σ_1 affinity but the highest uptake. Except for **12**, affinities for σ_2-receptors were at least 1 order of magnitude lower and also did not correlate with melanoma uptake. Thus, the inherent affinity of a given benzamide for σ-receptors is not an important determinant of melanoma uptake.

The expression of σ-receptors in the tumor model studied was evaluated by saturating B16 melanoma membranes with [^{3}H]-(+)-pentazocine (σ_1) and [^{3}H]DTG/dextrallorphan (σ_2). The K_d values of both receptors were found to be comparable with the K_d values found for the amelanotic melanoma A375.[13] However, the binding capacities in terms of the B_{max} values for both receptor types in B16 melanoma were 5−7 times higher than for the A375 tumor. We interpret this difference to be due to the additional interaction of [^{3}H]-(+)-pentazocine and [^{3}H]DTG with the melanin present in B16 melanoma.

In a recent clinical trial using [^{123}I]BZA,[7] which also exhibits high affinity for σ_1-receptors,[2] positive scintigraphic imaging of melanoma and metastases was achieved with specific activities as low as 0.006 GBq/μmol. For comparison, commercially available radiopharmaceuticals used for receptor imaging have specific activities of typically 15 or 200 GBq/μmol for [^{111}In]-pentetreotide or [^{123}I]IBZM, respectively. Therefore, saturation studies for B16 melanoma in the C57Bl/6 mouse model have been performed by injecting [^{131}I]-

IMBA and [^{131}I]BZA with specific activities ranging from 90 GBq/μmol (no carrier added) to 0.02 MBq/μmol (carrier added). As shown in Table 4 1- and 6-h tumor levels of [^{131}I]IMBA remained almost unchanged (nonsaturable) while the specificity (M/NTT) was reduced to some extent, not going below the values of BZA (see below). For [^{131}I]BZA a significant *increase* in melanoma uptake with decreasing specific activity and with time was observed. An increase at 6 h postinjection has also been detected with other radioiodinated benzamides.[5,6] In contrast to [^{131}I]IMBA the selectivity (M/NTT) of [^{131}I]-BZA *increased* with decreasing specific activity. These positive results at very low specific activities are consistent with the clinical studies mentioned above.

It is also interesting to note that radioiodinated 1-(iodopropen-2-yl)-4-[(4-cyanophenoxy)methyl]piperidine shows both high B16 melanoma uptake and high affinity for σ-receptors. However, melanoma uptake was not suppressed by DuP 734, a σ-receptor blocking agent, but was in fact doubled.[14] Thus, all of the results discussed in this section indicate that binding to σ-receptors is not an important mechanism for melanoma uptake of the compounds investigated here.

Role of Melanin. The intracellular distribution of [^{131}I]IMBA in the mouse model was investigated by analyzing homogenized B16 melanoma tissue by differential and density-gradient centrifugation techniques. In fractions obtained from differential centrifugation (Figure 2A) radioactivity peaked in pellet 3 (lysosomes, melanin granules). Following density-gradient centrifugation (Figure 2B) >60% of radioactivity was associated with fractions containing melanin granules, and an electron microscopy image (Figure 2C) showed dark-colored melanin granules in fraction 2 (Figure 2B). These studies demonstrated that there was no significant amount of membrane-bound radioactivity, and analysis of tissue extracts by HPLC indicated only the parent compound [^{131}I]IMBA, and not its metabolites, was responsible for the intracellular distribution observed.

Additional support for the binding of radioiodinated benzamides to melanin was recently obtained by others using B16/C3 melanoma cells.[15] Here, cellular uptake of [^{131}I]BZA was clearly dependent on the amount of melanin present in the cells.

Summary

The results of the experiments presented here provide strong evidence that the uptake of radioiodinated benzamides in B16 melanoma is not mediated by a specific uptake mechanism involving σ-receptors, for example, but is mainly controlled by the available vascular concentration of agent and diffusion or efficient transport into the melanoma cells. The binding sites are melanosomes, and the binding capacity appears to be nonsaturable, at least up to an injected dose of ca. 2 μmol/mouse. Similar characteristics were observed for other weak bases which concentrate in melanin-containing cells.[16] The SARs investigated here involve primarily metabolic stability and tissue and renal clearances which determine the local bioavailability of the diffusable benzamides in melanoma, their absolute uptake in tumor, and their differential clearance from tumor and nontarget tissues. The diagnostic value of [^{123}I]IMBA[5] or [^{123}I]BZA[7] is based on the relatively rapid clearance from nontarget tissue and the resulting high contrast for melanoma imaging within a few hours after injection. Of the new compounds presented here, **6** offers the highest potential for clinical use; it features highest melanoma uptake, slowest tumor washout, metabolic stability, and a moderate rate of clearance from most normal tissues (slow clearance from liver). This allows scintigraphic imaging with both high sensitivity (count rates) and high contrast to be achieved at 24 h postinjection, for example. In addition, at the uptake levels attained by **6**, radionuclide therapy with this agent may be feasible.

Materials and Methods

All commercially available chemicals were used without further purification. These include the following precursors: 4-amino-5-bromo-*N*-(2-diethylaminoethyl)-2-methoxybenzamide **(1)** (bromopride), 4-acetamido-*N*-(2-diethylaminoethyl)-benzamide **(8)** (*N*-acetylprocainamide), 3-methoxybenzoyl chloride **(10)** and 2-methoxybenzoyl chloride **(13)** (all from Sigma Aldrich, Deisenhofen, Germany); 4-amino-2-methoxybenzoate **(3)** prepared from 4-amino-2-hydroxybenzoic acid[17] (Lancaster; Mühlheim, Germany). $^{131}I^-$ with a specific activity of 90 GBq/μmol in 0.02 M NaOH was obtained from Amersham Int. (England). IMBA (*N*-(2-diethylaminoethyl)-3-iodo-4-methoxybenzamide), BZA (*N*-(2-diethylaminoethyl)-4-iodobenzamide), [^{131}I]BZA and [^{131}I]IMBA were prepared as described previously.[5] [^{3}H]-2-Dimethylallyl-5,9-dimethyl-2′-hydroxybenzomorphan ([^{3}H]-(+)-pentazocine; 1036 GBq/mmol) and [^{3}H]-1,3-di-*o*-tolylguanidine ([^{3}H]DTG; 1147 GBq/mmol) were obtained from NEN (Zaventem, Belgium). Melting points (mp) were determined in open capillary tubes using an electrothermal apparatus and are uncorrected. HPLC was carried out on LATEK systems equipped with variable UV (Latek, Heidelberg) and γ-radiation detectors (Berthold, Wildbad). The reverse-phase HPLC columns (270 × 4 mm) used were Nucleosil C_{18} 5 μm (Macherey & Nagel, Düren). The solvents used throughout for HPLC measurements consisted of MeOH and 0.9% TRIS buffer adjusted to pH 2.6 with H_3PO_4. The detectors were equipped with a C-R5A dual-channel integrator (Shimadzu, Duisburg).

Confirmation of the structures of the synthesized benzamides was obtained with the following analytical methods: MALDI-TOF mass spectrometry (MALDI I and III TOF spectrometer from Kratos/Shimadzu, Duisburg); elemental analysis (Microanalytical Laboratory, Chemistry Department, University of Heidelberg); ^{1}H and ^{13}C NMR spectroscopy at 7.0 T (Bruker AM-300 spectrometer, Rheinstetten, Germany). Signal assignments for the one-dimensional spectra could be made directly using chemical shift predictions based on (a) the empirical increment rules incorporated in the SpecTool software (version 2.1, Chemical Concepts, Weinheim, Germany) and (b) the experimental database in Bruker's SpecEdit software.

ESI-MS analyses of the urine metabolites were performed using a triple-quadrupole instrument (TSQ 7000 from Finnigan, San Jose, CA) equipped with a nanoelectrospray source (EMBL, Heidelberg). Samples were sprayed at ±600 V from gold-coated glass capillaries prepared in-house using a microcapillary puller (Sutter Instruments, type 87-B).[18] Argon was used as a collision gas at a nominal pressure of 2 mTorr.

4-Amino-5-bromo-*N*-(2-diethylaminoethyl)-3-iodo-2-methoxybenzamide (2). 218 mg (0. 0.633 mmol) of 4-amino-5-bromo-*N*-(2-diethylaminoethyl)-2-methoxybenzamide **(1)** was dissolved in 6 mL of TFA and reacted at ambient temperature with a 1.2-fold molar amount of $Tl(TFA)_3$. After 30 min 98.2 mg of NaI (0.655 mmol) in H_2O was added. The mixture was stirred at ambient temperature until the solid NaI dissolved and reacted with the thallated intermediate product. After 5 h TFA was evaporated and the residue dissolved in 6 mL of H_2O. The pH was raised above 12 with 10 M NaOH, and the

Table 5. ^{1}H NMR Data for Benzamides **2**−**15** as Free Bases in $CDCl_3$[a]

	^{1}H NMR chemical shifts in ppm relative to TMS (multiplicity)						
position[b]	**2**, 30 °C	**6**, 30 °C	**7**, 27 °C	**8**, 23 °C	**9**,[c] 30 °C	**12**, 27 °C	**15**, 27 °C
C2				7.712 (d)	8.281 (d)		
C3		8.224 (s, br)	6.274 (s)	7.608 (d)		7.694 (d)	6.728 (d)
C4						6.681 (dd)	7.688 (dd)
C5				7.608 (d)	8.300 (d, br)[e]		
C6	8.216 (s)	8.579 (s)	8.455 (s)	7.712 (d)	7.640 (dd)	6.985 (d)	8.476 (d)
N8	7.960 (t, br)	8.311 (t, br)	8.137 (t)	6.977 (t, br)	6.881 (t, br)	6.665 (br)	8.301 (t, br)
C9	3.510 (dt)	3.496 (dt)	3.477 (dt)	3.465 (dt)	3.446 (dt)	3.530 (dt)	3.507 (dt)
C10	2.641 (t)	2.620 (t)	2.607 (t)	2.639 (t)	2.632 (t)	2.721 (t)	2.633 (t)
C12	2.582 (q)	2.564 (q)	2.556 (q)	2.559 (q)	2.557 (q)	2.625 (q)	2.575 (q)
C13	1.034 (t)	1.041 (t)	1.034 (t)	1.033 (t)	1.031 (t)	1.061 (t)	1.045 (t)
4-NH_2	4.994 (s, br)		4.424 (s)				
4-NHAc (NH)		7.623 (s, br)		8.308 (s, br)	7.578 (s, br)		
(CH_3)		2.270 (s)		2.186 (s)	2.254 (s)		
OMe	3.803 (s)	3.960 (s)	3.868 (s)			3.794 (s)	3.924 (s)
J couplings[d]				8.7 (2, 3)	8.59 (5, 6)	8.75 (3, 4)	8.68 (3, 4)
					2.04 (2, 6)	3.0 (4, 6)	2.41 (4, 6)

[a] Free bases measured at 300 MHz at the temperatures given. [b] See Chart 1 for numbering. [c] For HCl salt at 45 °C, N11 is protonated and positively charged, giving a broad resonance at 11.45 ppm and the following characteristic shifts for the side chain: 8.955 (t, N8); 3.866 (dt, C9); 3.296 (dt, C10); 3.204 (dq, C12); 1.409 (t, C13). [d] In Hz with coupling partners in parentheses; couplings in the amide side chain are typically: 5.0 (8,9), 6.2 (9,10), 7.13 (12,13) in the free base and 4.4 (8,9), 6.0 (9,10), 4.5 (10,11), 4.5 (11,12), 7.27 (12,13) in the salt form. [e] Broad due to hindered rotation of the NHAc group.

solution was extracted twice with Et_2O. The organic phase was dried over Na_2SO_4 and evaporated. The residue was dissolved in methanolic HCl and evaporated. The oily residue crytallized slowly. Recrystallization from CH_2Cl_2/AcOEt yielded 249 mg of benzamide **2** (HCl salt) (78%). Mp: 128 °C. MALDI-MS: *m*/*z* 469.9, 471.9 $(M + H)^+$. Anal. ($C_{14}H_{22}BrClIN_3O_2$) C, H, N.

4-Acetamido-*N*-(2-diethylaminoethyl)-5-iodo-2-methoxybenzamide (6). 1.4 g (7.73 mmol) of methyl 4-amino-2-methoxybenzoate **(3)** (mp 157 °C; lit. mp 155−156 °C[17]) and 4.5 g (37.8 mmol) of 2-diethylaminoethylamine were heated at 90 °C for 12 h. Excess amine was evaporated under reduced pressure. Addition of 5 mL of 1 M NaOH (H_2O) and extraction with $CHCl_3$ afforded a slightly yellow oil after evaporation. Compound **4** was precipitated as the HCl salt in Et_2O (1.2 g, 54%). Mp: 164 °C (lit. mp 153 °C [19]). MALDI-MS: *m*/*z* 266.4 $(M + H)^+$. 400 mg (1.33 mmol) of compound **4** was transferred to the free base and dissolved in 10 mL of CH_3CN. Acetylation was performed at ambient temperature by the dropwise addition of 115 mg (1.46 mmol) of acetyl chloride. After 1 h the solvent was evaporated under reduced pressure. Addition of 3 mL of 1 M NaOH (H_2O) and extraction with $CHCl_3$ afforded compound **5** as a white, HPLC-pure solid (410 mg, ca. 100%). MALDI-MS: *m*/*z* 308.2 $(M + H)^+$. 350 mg (1.14 mmol) of compound **5** was dissolved in 20 mL of TFA and reacted with $Tl(TFA)_3/I^-$ as described for **2**. The benzamide **6** was precipitated as the free base and recrystallized from AcOEt/hexane (1/4) (245 mg, 50%). Mp: 120 °C. MALDI-MS: *m*/*z* 434.3 $(M + H)^+$. Anal. ($C_{16}H_{24}IN_3O_3$) C, H, N.

4-Amino-*N*-(2-diethylaminoethyl)-5-iodo-2-methoxybenzamide (7). 250 mg (0.828 mmol) of 4-amino-*N*-(2-diethylaminoethyl)-2-methoxybenzamide (HCl salt of **4**) was dissolved in 17 mL of 1 N HCl (H_2O) and mixed with 3.3 mL of 0.5 M KIO_3 (H_2O). To this solution was added 1.65 mL of 1 M NaI (H_2O) in 100-μL portions within 30 min. The resulting mixture was treated with 1.65 mL of 1 M $Na_2S_2O_5$ (H_2O) for 10 min and extracted with Et_2O after raising the pH above 12. After evaporation **7** was obtained as a slightly yellow oil which crystallized overnight. The solid was recrystallized from AcOEt (254 mg, 78%). Mp: 158 °C. MALDI-MS: *m*/*z* 392.2 $(M + H)^+$. Anal. ($C_{14}H_{22}IN_3O_2$) C, H, N.

4-Acetamido-*N*-(2-diethylaminoethyl)-3-iodobenzamide (9). 500 mg (1.8 mmol) of 4-acetamido-*N*-(2-diethylaminoethyl)benzamide **(8)** was dissolved in 36 mL TFA and reacted with $Tl(TFA)_3/I^-$ as described for **2**. Benzamide **9** was precipitated as the HCl salt and recrystallized from AcOEt (594 mg, 75%). Mp: 197−200 °C. MALDI-MS: *m*/*z* 404.4 $(M + H)^+$. Anal. ($C_{15}H_{23}ClIN_3O_2$) C, H, N.

***N*-(2-Diethylaminoethyl)-2-iodo-5-methoxybenzamide (12).** 400 mg (2.3 mmol) of 3-methoxybenzoyl chloride **(10)** was dissolved in 15 mL of CH_3CN and reacted with 293 mg (2.53 mmol) of 2-diethylaminoethylamine at ambient temperature for 2 h. Solvent and excess amine were evaporated under reduced pressure. Addition of 5 mL of 2 M NaOH (H_2O), extraction with $CHCl_3$, and evaporation of volatile components afforded compound **11** as a colorless oil (590 mg, ca. 100%). MALDI-MS: *m*/*z* 251.2 $(M + H)^+$. 500 mg (2.00 mmol) of the precursor **11** was dissolved in 40 mL of TFA and reacted with $Tl(TFA)_3/I^-$ as described for **2**. The crude product was precipitated as the HCl salt and recrystallized from AcOEt (759 mg, 80%). Mp: 178 °C. MALDI-MS: *m*/*z* 377.3 $(M + H)^+$. Anal. ($C_{14}H_{22}ClIN_2O_2$) C, H, N.

***N*-(2-Diethylaminoethyl)-5-iodo-2-methoxybenzamide (15).** 450 mg (2.64 mmol) of 2-methoxybenzoyl chloride (**13**) and 452 mg (3.9 mmol) 2-diethylaminoethylamine were reacted under comparable conditions, as described for **12**, to give compound **14** as a slightly yellow oil (665 mg, ca. 100%). MALDI-MS: *m*/*z* 251.2 $(M + H)^+$. 400 mg (1.6 mmol) of compound **14** was dissolved in 32 mL of TFA and reacted with $Tl(TFA)_3/I^-$ as described for **2**. The benzamide **15** was precipitated as the HCl salt and recrystallized from AcOEt (428 mg, 65%). Mp: 194−6 °C dec. MALDI-MS: *m*/*z* 377.3 $(M + H)^+$. Anal. ($C_{14}H_{22}ClIN_2O_2$) C, H, N.

Radioiodination of 2, 6, 9, 12, and 15 ($Tl(TFA)_3$/[^{131}I]-iodide method). The radiolabeling procedure has been described previously in detail.[5,6] Briefly, 20 μL of a 10 mM TFA solution of the corresponding precursor benzamide (**1**, **5**, **8**, **11** and **14**) was mixed with 10 μL of 10 mM $Tl(TFA)_3$ dissolved in TFA. After 10 min the solution was mixed with previously evaporated [^{131}I]iodide. After 5 min TFA was evaporated, and the resulting reaction mixture was separated on an analytical RP18 HPLC column using the following solvent gradient: 0−100% methanol in Tris buffer over 30 min at 0.7 mL/min. The collected eluate was evaporated to dryness, redissolved in 0.9% NaCl, neutralized and sterile-filtered. The radiochemical yields were 70−80% (isolated), and the specific activities of the no-carrier-added [^{131}I]benzamide preparations ranged between 70 and 90 GBq/μmol (calculated).

Radioiodination of 7 (KIO_3/[^{131}I]iodide method). Radiolabeling of **7** with ^{131}I was performed essentially as described earlier.[20] Briefly, 20 μL of a 10 mM solution of the precursor **4** (1 N HCl) was mixed with 5 μL of 50 mM KIO_3 (H_2O) and 30 MBq [^{131}I]iodide (0.02 M NaOH). After 10 min the reaction mixture was chromatographed by analytical HPLC (RP18 column) using a 0−100% methanol in TRIS buffer gradient over 30 min at 0.7 mL/min. The collected eluate was evaporated to dryness, redissolved in 0.9% NaCl (H_2O), neutralized and sterile-filtered. The radiochemical yield was 90% (isolated),

Table 6. ^{13}C NMR Data for Benzamides **2**−**15** as Free Bases in $CDCl_3$[a]

	^{13}C NMR chemical shifts in ppm relative to TMS (multiplicity)						
position[b]	**2**, 30 °C	**6**, 30 °C	**7**, 27 °C	**8**, 23 °C	**9**,[c] 30 °C	**12**, 27 °C	**15**, 27 °C
C1	117.48 (s)	119.11 (s)	114.26 (s)	129.90 (s)	131.85 (s)	143.13 (s)	124.02 (s)
C2	158.18 (s)	158.58 (s)	159.28 (s)	127.81 (d)	138.26 (d)	80.77 (s)	157.44 (s)
C3	80.94 (s)	103.95 (d)	96.79 (d)	119.24 (d)	89.31 (s, br) [e]	140.53 (d)	113.67 (d)
C4	147.96 (s)	141.44 (s)	150.30 (s)	141.11 (s)	140.70 (s)	117.69 (d)	140.94 (d)
C5	102.73 (s)	77.81 (s)	73.49 (s)	119.24 (d)	120.64 (d, br) [e]	159.79 (s)	83.56 (s)
C6	135.52 (d)	141.55 (d)	142.64 (d)	127.81 (d)	127.29 (d)	114.11 (d)	140.69 (d)
C7	163.43 (s)	163.35 (s)	164.04 (s)	166.91 (s)	165.08 (s)	169.07 (s)	163.64 (s)
C9	37.64 (t)	37.64 (t)	37.52 (t)	37.30 (t)	37.37 (t)	37.19 (t)	37.63 (t)
C10	51.53 (t)	51.48 (t)	51.66 (t)	51.18 (t)	51.22 (t)	51.32 (t)	51.41 (t)
C12	46.58 (t)	46.76 (t)	47.78 (t)	46.74 (t)	46.81 (t)	46.71 (t)	46.72 (t)
C13	11.66 (q)	12.16 (q)	12.15 (q)	12.05 (q)	12.07 (q)	11.45 (q)	12.05 (q)
4-NHAc (CO)		168.62 (s)		168.91 (s)	168.34 (s)		
(CH_3)		25.17 (q)		24.51 (q)	24.91 (q)		
OMe	61.89 (q)	56.07 (q)	55.73 (q)			55.52 (q)	55.96 (q)
$^1J_{CH}$[d]	168.9 (C6)	165.6 (C3) 168.9 (C6) 139.0 (C9) ca. 135 (C10) 132.0 (C12) 125.3 (C13) 128.7 (*Me*CO) 145.8 (OMe)	156.4 (C3) 166.7 (C6)		167.4 (C2) 161.0 (C6) ca. 169 (C5)	166.4 (C3) 162.0 (C4) 161.3 (C6)	160.5 (C3) 166.6 (C4) 168.8 (C6)
$^2J_{CH}$	1.9 (C1, H6) 4.0 (C5, H6) 3.9 (C7, NH)	1.9 (C1, H6) 4.0 (C2, H3) 4.0 (C4, H3) 6.3 (CO, Me) 2.5 (CO, 4-NH)	1.9 (C1, H6) 5.4 (C3, 4-NH_2) 2.2 (C4, H3) 6.5 (C5, 4-NH_2) 3.3 (C5, H6)			2.3 (C2, H3)	ca. 1 (C1, H6) ca. 1 (C3, H4) 3.0 (C5, H6) 3.0 (C5, H4)
$^3J_{CH}$	4.0 (C2, 2-OMe) 7.3 (C2, H6) 6.0 (C3, 4-NH_2) 8.5 (C4, H6) 6.2 (C5, 4-NH_2) 2.8 (C7, H9) 4.8 (C7, H6)	6.1 (C1, H3) 9.7 (C2, H6) 5.2 (C3, NHAc) 9.6 (C4, H6)	5.5 (C1, H3) 9.2 (C4, H6) 8.0 (C5, H3)		9.0 (C4, H2) 9.0 (C4, H6) 7.1 (C2, H6) 8.0 (C1, H5) 6.9 (C6, H2)	7.3 (C1, H3) 9.0 (C2, H6) 10.6 (C2, H4) 5.5 (C4, H6) 5.4 (C6, H4)	5.5 (C1, H3) 7.6 (C4, H6) 10.7 (C5, H3) 6.8 (C6, H4)
$^4J_{CH}$	1.8 (C3, H6)		1.0 (C3, H6)		0.8 (C2, H5)	1.4 (C6, H3)	ca. 1 (C1, H4) ca. 1 (C3, H6)

[a] Measured at 75.47 MHz at the temperatures given. [b] See Chart 1 for numbering. [c] For HCl salt (45 °C) protonation at N11 leads to characteristic changes in side chain shifts: 35.27 (t, C9); 52.75 (t, C10); 48.29 (t, C12); 8.62 (q, C13). [d] In Hz with coupling partners in parentheses. [e] Broad due to hindered rotation of NHAc group.

and the specific activity of the ^{131}I labeled **7** was 90 GBq/μmol (calculated).

Biodistribution Studies. The animal experiments were performed in compliance with the German Animal Protection Laws (Permission 37-9185.81/79/95, Reg.-Präsidium, Karlsruhe). Biodistribution time-course studies were performed with C57Bl/6 mice bearing the B16 murine melanoma. The tumor cells (DKFZ, Heidelberg) were washed with PBS and transplanted subcutaneously into the left flank by injecting 0.5×10^6 cells (0.1 mL). After 10−14 days each animal (20−29 g) was given an iv tail-vein injection of one of the ^{131}I-labeled benzamide derivatives (2−3 MBq dose). The injected volume was determined by weighing the syringe before and after injection. At specific times postinjection, the animals were weighed, sacrificed by cervical dislocation and dissected. Organs or tissues were blotted dry, when appropriate, and weighed. Radioactivities in tissues and in standards of the injected dose were determined with a γ-counter. The results (Table 1) are expressed as % ID/g tissue. In addition, a selectivity factor representing the mean melanoma/nontarget tissue ratio, M/NTT (averaged over all tissues examined), was calculated.

HPLC and ESI-MS/MS of Urinary Metabolites. 15 MBq of ^{131}I-labeled IMBA, BZA, **2**, **6** or **9** was intravenously injected into NMRI mice (29−33 g). After 4 h the excreted urine was collected and combined with the urine aspirated from the bladder. Radioactivity in the urine was counted, and the samples were chromatographed by RP-HPLC. In separate experiments a 1-mg sample of IMBA or BZA was injected into animals. The 4-h urine samples were desalted and used for negative-ion ESI-MS/MS.

Octanol/Buffer Partition Coefficients. The octanol/buffer partition coefficients were determined with HPLC-purified (no-carrier-added), radioiodinated benzamides. 10 μL of the HPLC eluate was transferred into 1 mL of 0.067 M phosphate buffer of pH 7.4. After the addition of 1 mL of 1-octanol the tubes were vortexed until equilibrium was reached. The emulsions were centrifuged and separated. Radioactivity in aliquots of each phase (100 μL) were measured in a γ-counter, and the partition coefficients are expressed as $\log P = \log(\mathrm{cpm}_{\mathrm{octanol}}/\mathrm{cpm}_{\mathrm{buffer}})$.

σ_1-Receptor Binding Assays. The in vitro σ_1 binding affinities of unlabeled benzamides were determined in a competition assay using guinea pig brain membranes and the high-affinity ligand [^{3}H]-(+)-pentazocine.[8] The membranes were prepared from guinea pig brains (minus cerebella) as previously described.[8] Fifteen concentrations of unlabeled benzamides ranging from 10^{-10} to 10^{-3} M and protein samples (0.15 mg of membrane protein) were incubated with 5 nM [^{3}H]-(+)-pentazocine in a total volume of 0.25 mL of 50 mM Tris-HCl, pH 8.0. Incubations were carried out for 120 min at 25 °C. The equilibrium binding constants (K_d and B_{max}) for the radioligand binding were determined using saturation binding assays with each assay tube containing 0.6−40 nM concentrations of [^{3}H]-(+)-pentazocine and 0.15 mg of protein in the same buffer volume as described above. Nonspecific binding was determined in the presence of 10 μM haloperidol and used for the correction of binding data. All assays were terminated by dilution with 5 mL of ice-cold 10 mM Tris-HCl, pH 8.0, and the solutions were filtered through glass fiber filters (Whatman GF/B; presoaked in 0.5% polyethylenimine for 30 min at 25 °C). Filters were then washed twice with 5 mL of

ice-cold 10 mM Tris-HCI, pH 8.0, and counted in Hionic-Fluor cocktail (Packard, Groningen, Netherlands). The corresponding IC_{50}, K_d and B_{max} values were determined using SigmaPlot software (SigmaPlot 4.0, SPSS Inc., Chicago, IL) and were used for the calculation of the apparent K_i values.[10]

σ_2-Receptor Binding Assays. Rat liver membranes were prepared from the livers of male Sprague−Dawley rats as previously described.[9] The σ_2-receptors were labeled as previously described[9] using [^{3}H]DTG as ligand in the presence of 1 μM dextrallorphan to mask σ_1-receptors. Competition assays were performed with 15 concentrations of unlabeled benzamides ranging from 10^{-10} to 10^{-3} M and protein samples (0.10 mg of membrane protein) in 50 mM Tris-HCI, pH 8.0, for 120 min at 25 °C in a volume of 0.25 mL. The equilibrium binding constants (K_d and B_{max}) for the radioligand binding were determined as described above using saturation binding assays with each assay tube containing 0.6−80 nM concentrations of [^{3}H]-(+)-pentazocine and 0.1 mg of protein in the buffer volume described above. Nonspecific binding was determined in the presence of 10 μM haloperidol. All other manipulations and data analysis were performed as described above for the σ_1-receptor assay.

Saturation Assays for B16 Membranes. B16 melanoma membranes were prepared from subcutaneously transplanted B16 cells (2×10^6 cells/mouse) grown for 10 days in C57Bl/6 mice. The preparation conditions of the membranes were adapted to the procedures described earlier.[8,9] Binding studies for σ_1- and σ_2-receptors in B16 melanoma membranes were carried out under the conditions described above. Twelve concentrations of the radioligands [^{3}H]-(+)-pentazocine and [^{3}H]DTG (in the presence of 1 μM dextrallorphan) in the range 1−80 nM were applied. Nonspecific binding was determined in the presence of 10 μM haloperidol. All other manipulations and data analysis were performed as described above for the σ_1-receptor assay.

Density-Gradient Ultracentrifugation of B16 Homogenate and Ultrastructural Analysis. One hour after injection of radiolabeled benzamide, the B16 tumor was dissected and homogenized at 4 °C using a glass−Teflon Potter homogenizer rotating at 800 min^{-1}. Differential centrifugation of the homogenated tissue produced four pellets which consisted of crudely separated cell organelles, as outlined in Figure 2A. Subcellular fractionation of the B16 homogenate was carried out essentially as described previously for the separation of a rat liver light mitochondrial fraction.[21] Briefly, pellets 2 and 3 obtained from differential centrifugation were layered on top of a density gradient made up of 30−70% (w/v) Nycodenz overlayed with a reversed sucrose gradient of 8−0% (w/v) in 10 mM glycylglycine (pH 7.4), 1 mM EDTA and 0.1% ethanol. Centrifugation was performed in a vertical rotor at 30000*g* for 90 min at 4 °C. Fractions were recovered from bottom to top and counted in a γ-counter. For electron microscopy organelle fractions were diluted, pelleted, and fixed with 2.5% glutaraldehyde in 0.1 M cacodylate buffer (pH 7.4). Subsequently the fixed organelle pellets were embedded in Epon as decribed previously.[22] Ultrathin sections were viewed in an EM 10 electron microscope (Zeiss, Oberkochen, Germany).

Acknowledgment. A postdoctoral grant for A.M. and a research grant, both received from the Deutsche Forschungsgemeinschaft (DFG), are gratefully acknowledged. We also thank Dr. K. C. Rice (NIH, Bethesda, MD) as well Dr. E.-M. Gutknecht, P. Weber, and Dr. S. Hauptmann (Roche-Pharma, Basel, Switzerland) for generous gifts of dextrallorphan.

References

(1) Michelot, J. M.; Moreau, M. F. C.; Labarre, P. G.; Madelmont, J. C.; Veyre, A. J.; Papon, J. M.; Parry, D. F.; Bonafous, J. F.; Boire, J. Y. P.; Desplanches, G. G.; Bertrand, S. J.; Meyniel, G. Synthesis and evaluation of new ^{125}I radiopharmaceuticals as potential tracers for malignant melanomas. *J. Nucl. Med.* **1991**, *32*, 1573−1580.

(2) John, C. S.; Bowen, W. D.; Saga, T.; Kinuya, S.; Vilner, B. J.; Baumgold, J.; Paik, C. H.; Reba, R. C.; Neuman, R. D.; Varma, V. M.; McAfee J. G. A malignant melanoma imaging agent. Synthesis, characterization, in vitro binding and biodistribution of 4-[^{125}I]iodo-(2-piperidinylaminoethyl)benzamide. *J. Nucl. Med.* **1993**, *34*, 2169−2175.

(3) Moreau, M. F.; Michelot, J.; Papon, J. M.; Bayle, M.; Labarre, P. G.; Madelmont, J. C.; Parry, D. F.; Boire, J. Y. P.; Moins, N.; Seguin, H.; Veyre, A. J.; Mauclaire L. Synthesis, radiolabeling, and preliminary evaluation in mice of some (*N*-diethylaminoethyl)-4-iodobenzamide derivatives as melanoma imaging agents. *Nucl. Med. Biol.* **1995**, *22*, 737−747.

(4) Brandau, W.; Niehoff, T.; Pulawski, P.; Jonas, M.; Dutschka, K.; Sciuk, J.; Coenen, H. H.; Schober, O. Structure distribution relationship of I-123 iodobenzamides as tracers for the detection of melanotic melanoma. *J. Nucl. Med.* **1996**, *37*, 1865−1871.

(5) Nicholl, C.; Mohammed, A.; Hull, W. E.; Bubeck, B.; Eisenhut, M. Pharmacokinetics of ^{123}I-IMBA for melanoma imaging. *J. Nucl. Med.* **1997**, *38*, 127−133.

(6) Mohammed, A.; Nicholl, C.; Titsch U.; Eisenhut, M. Radioiodinated *N*-(alkylaminoalkyl)-substituted 4-methoxy-, 4-hydroxy-, and 4-aminobenzamides: biological investigations for the improvement of melanoma-imaging agents. *Nucl. Med. Biol.* **1997**, *24*, 373−380.

(7) Michelot, J. M.; Moreau, M. F. C.; Veyre, A. J.; Bonafous, J. F.; Bacin, F. J.; Madelmont, J. C.; Bussiere, F.; Souteyrand, P. A.; Mauclaire, L. P.; Chossat, F. M.; Papon, J. M.; Labarre, P. G.; Kauffmann, P.; Plagne, R. J. Phase II scintigraphic clinical trial of malignant melanoma with iodine-123-*N*-(2-diethylaminoethyl-4-iodobenzamide). *J. Nucl. Med.* **1993**, *34*, 1260−1266.

(8) Bowen, W. D.; de Costa, B. R.; Hellewell, S. B.; Walker J. M.; Rice, K. C. [^{3}H]-(+)-Pentazocine: a potent and highly selective benzomorphan-based probe for sigma-1 receptors. *Mol. Neuropharmacol.* **1993**, *3*, 117−126.

(9) Hellewell S. B.; Bruce A.; Feinstein G.; Orringer J.; Williams W.; Bowen W. D. Rat liver and kidney contain high densities of σ_1 and σ_2 receptors: characterization by ligand binding and photoaffinity labeling. *Eur. J. Pharmacol.-Mol. Pharmacol. Sect.* **1994**, *268*, 9−18.

(10) Cheng, Y.; Prusoff, W. H. Relationship between the inhibition constant (K_I) and the concentration of inhibitor which causes 50% inhibition (IC_{50}) of an enzymatic reaction. *Biochem. Pharmacol.* **1973**, *22*, 3099−3108.

(11) Menon, I. A.; Haberman, H. F. Isolation of melanin granules. *Methods Enzymol.* **1974**, *31* (Part A), 389−394.

(12) John, C. S.; Bowen, W. D.; Fisher, S. J.; Lim, B. B.; Geyer, B. C.; Vilner, B. J.; Wahl, R. L. Synthesis, in vitro pharmacologic characterization, and preclinical evaluation of *N*-[2-(1′-piperidinyl)ethyl]-3-[125I]iodo-4-methoxybenzamide (P[125I]MBA) for imaging breast cancer. *Nucl. Med. Biol.* **1999**, *26*, 377−382.

(13) Vilner, B. J.; John, C. S.; Bowen, W. D. Sigma-1 and sigma-2 receptors are expressed in a wide variety of human and rodent tumor cell lines. *Cancer Res.* **1995**, *55*, 408−413.

(14) Waterhouse, R. N.; Chapman, J.; Izard, B.; Donald, A.; Belbin, K.; O'Brian, J. C.; Collier, T. L. Examination of four ^{123}I-labeled piperidine-based sigma receptor ligands as potential melanoma imaging agents: Initial studies in mouse tumor models. *Nucl. Med. Biol.* **1997**, *24*, 587−593.

(15) Dittmann, H.; Coenen, H. H.; Zolzer F.; Dutschka K.; Brandau W.; Streffer C. In vitro studies on the cellular uptake of melanoma imaging aminoalkyl-iodobenzamide derivatives (ABA). *Nucl. Med. Biol.* **1999**, *26*, 51−56.

(16) El Gamoussi, R.; Threadgill, M. D.; Prade, M.; Stratford, I. J.; Guichard, M. Relationship between the melanin content of a human melanoma cell line and its radiosensitivity and uptake of pimonidazole. *Cancer Chemother. Pharmacol.* **1993**, *31*, 277−282.

(17) Murakami, M.; Inukai, N.; Koda A.; Nakano K. An improved synthesis of metoclopramide. *Chem. Pharm. Bull.* **1971**, *19*, 1696−1699.

(18) Wilm, M.; Mann, M. Analytical properties of the nanoelectrospray ion-source. *Anal. Chem.* **1996**, *68*, 1−8.

(19) Thominet, M. L. Compositions for treatment of emesis and behavior disturbances. U.S. Patent 3,219,528, 1965; *Chem. Abstr.* **1966**, *64*, 12609h.

(20) Bubeck, B.; Eisenhut, M.; Heimke, U.; zum Winkel, K. Melanoma affine radiopharmaceuticals. I. A comparative study of ^{131}I-labeled quinoline and tyrosine derivatives. *Eur. J. Nucl. Med.* **1981**, *6*, 227−233.

(21) Hartl, F. U.; Just, W. W. Integral membrane polypeptides of rat liver peroxysomes: Topology and response to different metabolic states. *Arch. Biochem. Biophys.* **1987**, *255*, 109−119.

(22) Gorgas, K. Serial section analysis of mouse hepatic peroxysomes. *Anat. Embryol.* **1985**, *172*, 21−32.

JM991079P